Increased Monomolecular Recombination in MOCVD Grown 1.3-μm InGaAsN–GaAsP–GaAs QW Lasers From Carrier Lifetime Measurements

O. Anton, C. S. Menoni, J. Y. Yeh, L. J. Mawst, J. M. Pikal, and N. Tansu

***Abstract*—The recombination lifetime of metal–organic chemical vapor deposition grown InGaAsN–GaAsP–GaAs lasers with nitrogen content of 0% and 0.5% has been investigated from below threshold modulation frequency response measurements. Using an analysis that removes the contribution of electrical parasitic effects from the measured lifetime, it is shown that the recombination lifetime is significantly reduced when nitrogen is added into the quantum well. Furthermore, it is shown that this reduction is mainly the result of approximately a factor of four increase in the monomolecular recombination rate.**

***Index Terms*—InGaAsN, laser diodes.**

I. Introduction

In THE last few years, a new path in the engineering of 1.3-μm lasers for communications has been pursued with the development of alloys based on the InGaAsN–GaAs system. Bandgap engineering on GaAs alloys with incorporation of nitrogen and strain has provided wavelengths of around 1.3 μm and promises even longer wavelengths by further controlling the strain [1], [2]. The advantage of the GaInAs-based alloys compared with their InP counterpart lies in the increased electron confinement, and in the possibility of grow on GaAs substrates. Band structure modification with nitrogen has been predicted to impact the device's differential gain (dg/dN), frequency bandwidth, and T_o, the characteristic parameter that plays a fundamental role in the temperature sensitivity of the laser threshold current [3]. Key to understanding the impact of the incorporation of nitrogen on the device output, and its temperature sensitivity, is to investigate the mechanisms that control carrier recombination.

In this letter, we report on the first direct observation by carrier lifetime measurements that the incorporation of 0.5% of nitrogen leads to a four-fold increase in the monomolecular recombination. Carrier recombination was investigated from the behavior of the differential carrier lifetime with carrier density on two identical $InGaAs_{1-x}N_x$ laser diodes, that differ only in the nitrogen content x in the well. The differential carrier lifetime (τ) was determined at 20 °C from small signal frequency response measurements on lasers biased from 0.2 A/cm^2 to threshold. Using a rate equations analysis that incorporates electrical parasitic effects arising from the device junction, we obtained the carrier density in the laser active region at each bias and the effective A, B, and C recombination parameters for the InGaAs and the InGaAsN lasers.

Manuscript received October 12, 2004; revised December 20, 2004. This work was supported by National Science Foundation (NSF) Grant ECS 03 134 410. The work of O. Anton was supported by an Agilent Photonics Fellowship. The work of J. Pikal was supported by the Army Research Office (ARO) under Contract DAAD19-01-1-0567.

O. Anton and C. S. Menoni are with the Department of Electrical and Computer Engineering, Colorado State University, Fort Collins, CO 80523-1373 USA (e-mail: anton@engr.colostate.edu; carmen@engr.colostate.edu).

J. Y. Yeh and L. J. Mawst are with Reed Center for Photonics, Department of Electrical Computer Engineering, University of Wisconsin, Madison, Madison, WI 53706-1691 USA (e-mail: jyeh@cae.wisc.edu; mawst@engr.wisc.edu).

J. M. Pikal is with the Department of Electrical and Computer Engineering, University of Wyoming, Laramie, WY 82071 USA (e-mail: jpikal@uwyo.edu).

N. Tansu is with the Center for Optical Technologies, Department of Electrical and Computer Engineering, Sinclair Laboratory, Lehigh University, Bethlehem, PA 18015 USA (e-mail: Tansu@Lehigh.Edu).

Digital Object Identifier 10.1109/LPT.2005.844332

II. Experiments

Subthreshold frequency response measurements versus bias current were conducted on two identical $In_{0.4}Ga_{0.6}As_{1-x}N_x$ single quantum-well (QW) lasers with $x = 0$ and $x = 0.005$. The two device structures are grown by metal–organic chemical vapor deposition (MOCVD) [1] and consist of a single QW of width $L_a = 60$ Å, which is surrounded by two tensile strain $GaAs_{0.85}P_{0.15}$ barriers, and 100-Å GaAs spacers in between them. This structure is embedded in a 3000-Å GaAs separate confinement region followed by the p^+ and n^+ AlGaAs claddings, which form the laser diode. The InGaAs and InGaAsN broad area devices feature a 100-μm-wide stripe and lengths of 750 and 1000 μm, respectively. The InGaAs and InGaAsN laser emissions occur at 1.2 and 1.3 μm, with threshold currents of 125 and 256 A/cm^2, respectively.

The setup for the frequency response measurements at low biases comprises the laser and a radio-frequency (RF) probe of impedance r_p driven by an Agilent 8753 vector network analyzer (VNA) [4]. The VNA combines the frequency swept sine wave with the dc bias current. The laser output is measured by an avalanche photodiode whose output signal is connected to an amplifier and then to the input port of the VNA. For bias currents exceeding 30 A/cm^2, we implemented a variation in the setup that allowed measuring the frequency response under pulse bias. This was needed to reduce the Joule heating that might affect the laser frequency response, thus assuring that all measurements were conducted at a constant active area temperature of 20 °C. The frequency of the sine wave is swept from 0.1 MHz to 1 GHz at an amplitude level that produces a modulation index of 5% or less in the laser current to insure small signal modulation.

III. Results and Analysis

Fig. 1 shows the frequency response traces obtained in InGaAs and InGaAsN laser structures at bias current densities of

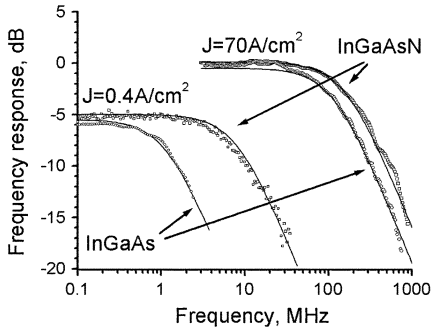

Fig. 1. (a) Frequency response of InGaAs and InGaAsN laser diodes at $J = 0.4$ and $J = 70$ A/cm^2. The solid lines are the fit of data with a single pole response function.

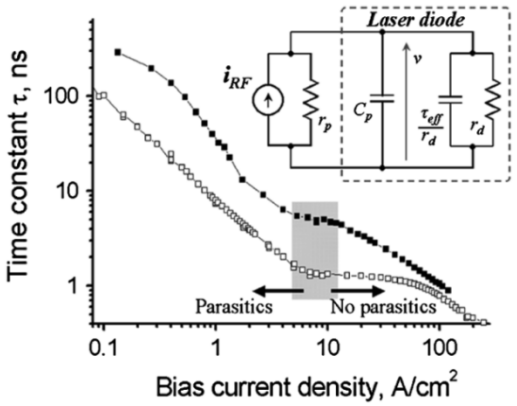

Fig. 2. Characteristic time constant $\tau = 1/2\pi f_{3\ \mathrm{dB}}$ plotted versus current density J up to threshold. The shaded rectangle separates the regions where the lifetime is dominated by the parasitic (left) or by the carrier recombination lifetime (right). The inset on top shows a schematic of the equivalent circuit of the laser diode representing (1).

0.4 and 70 A/cm^2. These traces are representative of the behavior observed at all biases. The traces present a single dominant pole $1/2\pi\tau$, whose characteristic time τ is extracted by minimum squares fit.

Fig. 2 plots τ versus the bias current density J for both lasers. Two different features are observed: 1) τ is smaller in the InGaAsN than in InGaAs lasers, and 2) after looking like it may saturate at around 10 A/cm^2, the lifetime then continues to increase as the bias reduces further. The former suggests that carrier recombination is increased in the dilute nitride lasers. The latter indicates that τ in this range is affected by the device parasitics.

The analysis of the lifetime versus current density behavior of Fig. 2 was carried out using a modified rate equation analysis which includes electrical parasitics [5], [6]. These equations correspond to an equivalent circuit of the laser diode and parasitics as shown in the inset of Fig. 2. The analysis assumes that part of the injected current i_{RF} is shunted through the parasitic components r_p and C_p, as explicitly shown in (1). We also assume that the current which reaches the active region all recombines in the well.[1] In this case, the small signal rate of change $\dot{n}$ and $\dot{n}_p$ of the active area carrier (n), and photon (n_p) densities are expressed as

$$\dot{n}(t) = \frac{\eta_{\mathrm{inj}}}{qV_a}\left[i_{\mathrm{RF}}(t) - \frac{v(t)}{r_p} - C_p\dot{v}(t)\right] - \frac{n}{\tau_{\mathrm{eff}}}$$
$$\dot{n}_p(t) = \beta\frac{n(t)}{\tau_{\mathrm{eff}}} - \frac{n_p}{\tau_p}. \quad (1)$$

In (1), $V_a = 4.5\times10^{-10}(6\times10^{-10})$ cm^3 is the active area volume, $\eta_{\mathrm{inj}} = 0.81(0.67)$ is the injection efficiency [7], q the electron charge, and $\tau_p = 4.8(5.7)$ ps is the photon lifetime for InGaAs (InGaAsN), respectively. τ_{eff} is the effective differential carrier recombination lifetime and β is the spontaneous emission factor. The electrical parasitics are represented in (1) by the capacitance C_p connected in parallel to the laser contacts and resistor r_p. C_p lumps the oxide layer and junction capacitances of the device and it shunts part of the modulation current $i_{\mathrm{RF}}(t)$. $i_{\mathrm{RF}}(t)$ represents the total probe short circuit current and $v(t)$ is the small signal variation of the laser contacts' voltage V. Assuming Boltzmann statistics for the carriers in the laser active region and flat-band conditions, V corresponds to the quasi-Fermi levels separation and, thus, $[N+n(t)] \prec \exp[(V+v(t))/k_BT]$ [8], where N and k_B are the steady state carrier density in the active area and Boltzmann constant, respectively. When linearizing (1) for small signal conditions, $v(t)$ becomes proportional to $n(t)$. Therefore, we substituted $n(t)qV_ar_d/(\eta_{\mathrm{inj}}\tau_{\mathrm{eff}})$ for $v(t)$ in (1), where r_d is the diode differential resistance. A similar substitution is made for $\dot{v}(t)$. The solution of (1) yields a dominant pole $1/2\pi\tau$, which contains the lifetime τ_{eff}, and the electrical parasitics. In the limit of $r_p \to \infty, \tau$ can be expressed as a function of τ_{eff}, r_d, and C_p, as

$$\tau = \tau_{\mathrm{eff}} + r_d \cdot C_p. \quad (2)$$

In other words, (2) predicts that τ does not saturate at low currents but rather that it continues to increase due to the $r_d \cdot C_p$ term. This behavior is observed in the experimental data of Fig. 2, for currents below ~7–10 A/cm^2. Therefore, to remove this effect, we fit τ/r_d in the InGaAs and InGaAsN lasers only above 7–10 A/cm^2.

To extract the dependence of τ_{eff} on carrier density and related recombination parameters A, B, and C, we simultaneously fitted $\tau_{\mathrm{eff}}(N)$ and current density $J(N)$ given by the traditional polynomial expression [6]

$$\frac{1}{\tau_{\mathrm{eff}}} = A + 2BN + 3CN^2 \quad (3)$$
$$J = \frac{q\cdot L_a}{\eta_{\mathrm{inj}}}(AN + BN^2 + CN^3) = J_A + J_B + J_C. \quad (4)$$

In (4), J_A, J_B, and J_C are the contributions to the current associated with each of the recombination terms. The values of A, B, and C obtained from the fit, assuming η_{inj} to be bias independent, are summarized in Table I. The results of the fit allowed extraction of A with an uncertainty of 5%–10% and C with an uncertainty of 20%–40%. However, the fit was not sensitive to

[1]This assumption is based on a fast carrier capture and slow escape rates, consistent with increased carrier confinement. This is experimentally confirmed through photoluminescence measurements, where the barrier integrated emission is 0.5% of that of the well.

TABLE I
A, B, AND C PARAMETERS RETRIEVED FROM THE FIT OF $\tau_{\text{eff}}(J)$. FIT IS NOT SENSITIVE TO B FOR EITHER InGaAs OR InGaAsN LASERS

Structure	A [s^{-1}]	B [$cm^3 s^{-1}$]	C [$cm^6 s^{-1}$]
$In_{0.40}Ga_{0.60}As$	$2.1\cdot10^{8}$	$<10^{-13}$	$7.7\cdot10^{-29}$
$In_{0.4}Ga_{0.6}As_{0.995}N_{0.005}$	$7.7\cdot10^{8}$	$<10^{-13}$	$3.1\cdot10^{-28}$

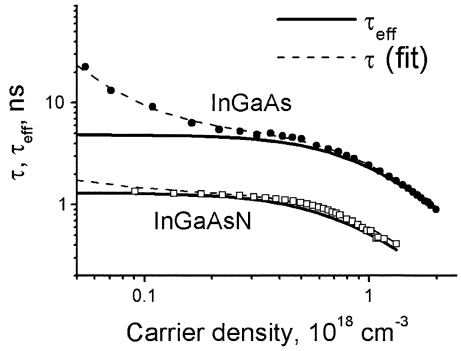

Fig. 3. τ and τ_{eff} versus N based on the A, B, and C parameters of Table I. The dashed lines are the result of the fit with the solution of (1). The solid lines identify the "parasitic-free" solution of (1) that yields the differential carrier recombination lifetime.

B, mainly because after removing the region dominated by parasitics there was only one decade left in current from which to extract the recombination parameters. This also contributes to the larger uncertainty in C. It is important to note that a bias dependent η_{inj} would affect C more than the linear term A in (3). This coupled with the larger uncertainty in the extraction of C from the fit does not allow us to draw significant conclusions about the differences in C between the two structures. This is not the case for A, where the analysis conclusively shows an increase of approximatley a factor of four in A with the incorporation of 0.5% of nitrogen in the well material. The increase in A, usually attributed to the monomolecular recombination coefficient, is likely to originate from increased contribution of defect recombination with increased nitrogen content in the well [5], [9], [10].

The plot of τ versus N in Fig. 3 distinctively shows the contribution of A, evidenced by the constant behavior of $\tau_{\text{eff}}(N)$, for $N = (2\text{–}4)\times10^{17}$ cm^{-3} for InGaAsN and $N = (2.5\text{–}5)\times10^{17}$ cm^{-3} for InGaAsN. The figure also shows the rapid reduction of τ_{eff} due to the contribution of the $1/CN^2$ term above $N = 9\times10^{17}$ cm^{-3} and $N = 6\times10^{17}$ cm^{-3} for InGaAs and InGaAsN, respectively.

The contributions of J_A and J_C to J are shown in Fig. 4 for the InGaAs and InGaAsN lasers. The figure reveals that over the entire range of biases, J_A is dominant in the InGaAsN lasers, but as threshold is approached J_C plays a comparable role. Surprisingly, J_A also plays an important role in the recombination of InGaAs. This may be a result of higher defect incorporation in the InGaAs active layer which is grown at a low temperature (530 °C). These results are good agreement with recent work by Tomic *et al.*, [3] that show the monomolecular, radiative, and Auger currents account for 55%, 20%, and 25% of the total current in the nitrogen containing alloys at room temperature.

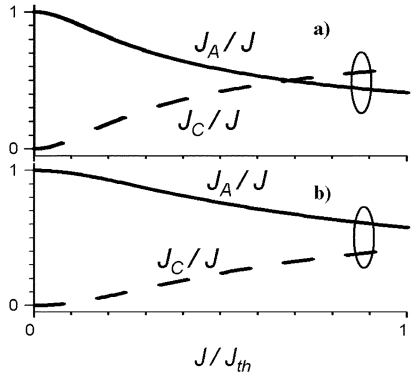

Fig. 4. Contribution of J_A (solid line) and J_C (dotted line) to the total current J for (a) InGaAs and (b) InGaAsN lasers.

IV. CONCLUSION

From small signal frequency response measurements and an analysis that separates the contribution of electrical parasitics, we have obtained the differential carrier lifetime and its dependence on carrier density in InGaAs and InGaAsN QW laser diodes. These results show that the incorporation of 0.5% nitrogen, necessary to reach the benchmark output wavelength of 1.3 μm, significantly reduces the differential carrier recombination lifetime. This is found to be mainly due to a factor of four increase in the monomolecular recombination term. This increase in A is likely the result of increased defect recombination in the nitrogen containing alloy.

REFERENCES

[1] N. Tansu and L. J. Mawst, "Low-threshold strain-compensated InGaAs(N) (lambda = 1.19–1.31 mu m) quantum-well lasers," *IEEE Photon. Technol. Lett.*, vol. 14, no. 4, pp. 444–446, Apr. 2002.

[2] D. Gollub, S. Moses, A. Fischer, M. Kamp, and A. Forchel, "GaInNAs-based distributed feedback laser diodes emitting at 1.5 mu m," *Electron. Lett.*, vol. 40, pp. 427–428, 2004.

[3] S. Tomic, E. P. O'Reilly, R. Fehse, S. J. Sweeney, A. R. Adams, A. D. Andreev, S. A. Choulis, T. J. C. Hosea, and H. Riechert, "Theoretical and experimental analysis of 1.3-mu m InGaAsN/GaAs lasers," *IEEE J. Sel. Topics Quantum Electron.*, vol. 9, no. 5, pp. 1228–1238, Sep./Oct. 2003.

[4] J. M. Pikal, C. S. Menoni, H. Temkin, P. Thiagarajan, and G. Y. Robinson, "Impedance independent optical carrier lifetime measurements in semiconductor lasers," *Rev. Sci. Instruments*, vol. 69, pp. 4247–4248, 1998.

[5] R. Olshansky, C. B. Su, J. Manning, and W. Powazinik, "Measurement of radiative and nonradiative recombination rates in InGaAsP and AlGaAs light-sources," *IEEE J. Quantum Electron.*, vol. QE-20, no. 8, pp. 838–854, Aug. 1984.

[6] J. M. Pikal, C. S. Menoni, H. Temkin, P. Thiagarajan, and G. Y. Robinson, "Carrier lifetime and recombination in long-wavelength quantum-well lasers," *IEEE J. Sel. Topics Quantum Electron.*, vol. 5, no. 3, pp. 613–619, May/Jun. 1999.

[7] J. Y. Yeh, N. Tansu, and L. J. Mawst, "Temperature-sensitivity analysis of 1360-nm dilute-nitride quantum-well lasers," *IEEE Photon. Technol. Lett.*, vol. 16, no. 3, pp. 741–743, Mar. 2004.

[8] I. Esquivias, S. Weisser, B. Romero, J. D. Ralston, and J. Rosenzweig, "Carrier dynamics and microwave characteristics of GaAs-based quantum-well lasers," *IEEE J. Quantum Electron.*, vol. 35, no. 4, pp. 635–646, Apr. 1999.

[9] A. Y. Polyakov, N. B. Smirnov, A. V. Govorkov, A. E. Botchkarev, N. N. Nelson, M. M. E. Fahmi, J. A. Griffin, A. Khan, S. N. Mohammad, D. K. Johnstone, V. T. Bublik, K. D. Chsherbatchev, and M. Voronova, "Interface properties and deep levels in InGaAsN/GaAs and GaAsN/GaAs heterojunctions," *Solid-State Electron.*, vol. 46, pp. 2141–2146, 2002.

[10] C. H. Fischer and P. Bhattacharya, "Photoluminescence and deep levels in lattice-matched InGaAsN/GaAs," *J. Appl. Phys.*, vol. 96, pp. 4176–4180, 2004.